

# NJC

New Journal of Chemistry

Accepted Manuscript

A journal for new directions in chemistry

This article can be cited before page numbers have been issued, to do this please use: B. Zhang, X. Liu, H. Xiong, Q. Zhang, X. Sun, Z. Yang, S. Xu, P. Zheng and W. Zhu, *New J. Chem.*, 2020, DOI: 10.1039/D0NJ00575D.



This is an Accepted Manuscript, which has been through the Royal Society of Chemistry peer review process and has been accepted for publication.

Accepted Manuscripts are published online shortly after acceptance, before technical editing, formatting and proof reading. Using this free service, authors can make their results available to the community, in citable form, before we publish the edited article. We will replace this Accepted Manuscript with the edited and formatted Advance Article as soon as it is available.

You can find more information about Accepted Manuscripts in the [Information for Authors](#).

Please note that technical editing may introduce minor changes to the text and/or graphics, which may alter content. The journal's standard [Terms & Conditions](#) and the [Ethical guidelines](#) still apply. In no event shall the Royal Society of Chemistry be held responsible for any errors or omissions in this Accepted Manuscript or any consequences arising from the use of any information it contains.

**Discovery of [1,2,4]triazolo[4,3-*a*]pyrazine derivatives bearing 4-oxo-pyridazinone moiety as potential c-Met kinase inhibitors**

Binliang Zhang <sup>a, 1</sup>, Xiaobo Liu <sup>a, 1</sup>, Hehua Xiong <sup>a</sup>, Qian Zhang <sup>a</sup>, Xin Sun <sup>a</sup>, Zunhua Yang <sup>b</sup>, Shan Xu <sup>a</sup>, Pengwu Zheng <sup>a, \*</sup> and Wufu Zhu <sup>a, \*</sup>

<sup>a</sup> Jiangxi Provincial Key Laboratory of Drug Design and Evaluation, School of Pharmacy, Jiangxi Science & Technology Normal University, 605 Fenglin Road, Nanchang, Jiangxi 330013, China

<sup>b</sup> College of Pharmacy, Jiangxi University of Traditional Chinese Medicine, Nanchang, 330004, China

\* Corresponding author.

Tel. & Fax: +86 791 8380-2393;

E-mail: zhengpw@126.com (P. Zheng), zhuwufu-1122@163.com (W. Zhu)

**Abstract:**

Two series of [1,2,4]triazolo[4,3-*a*]pyrazine derivatives bearing 4-oxo-pyridazinone moiety (compounds **21a-l** and **22a-l**) were designed and evaluated for the IC<sub>50</sub> values against three cancer cell lines (A549, MCF-7 and Hela) and c-Met kinase. Among them, the most potential compound **22i** exhibited excellent anti-tumor activity against A549, MCF-7 and Hela cancer cell lines with IC<sub>50</sub> values of 0.83 ± 0.07 μM, 0.15 ± 0.08 μM and 2.85 ± 0.74 μM, respectively, and also possessed superior c-Met kinase inhibition at nanomolar level (IC<sub>50</sub> = 48 nM). Moreover, dose-dependent experiments, AO fluorescence staining, cell cycle assay, Annexin V-FITC/PI staining and docking studies were carried out in this study. The results demonstrated that the compound **22i** could be a potential c-Met kinase inhibitor.

**Keywords:** [1,2,4]Triazolo[4,3-*a*]pyrazine; c-Met inhibitors; 4-oxo-pyridazinone; Anti-tumor activity<sup>□</sup>

\* Corresponding author. Tel./fax: +86 791 83802393.

<sup>1</sup> These authors contribute equally to this work.

E-mail address: zhengpw@126.com (P. Zheng), zhuwufu-1122@163.com (W. Zhu).

## 1 Introduction

HGF/c-Met signaling plays a prominent role in tumor growth, invasion, proliferation and angiogenesis, which has been identified as a promising target for the treatment of cancer, providing an effective therapeutic target for malignancy<sup>1-2</sup>. At present, two drugs namely Crizotinib and Cabozantinib had been approved by FDA<sup>3-4</sup>. Moreover, there are also many c-Met inhibitors undergoing clinical trial or preclinical research, such as Foretinib<sup>5</sup>, AMG337<sup>6</sup> and so on (**Figures 1 and 2**). According to their structures and their binding models with c-Met kinase, the reported c-Met inhibitors are mainly summarized and classified into Class I (e.g. AMG337), Class II (e.g. Foretinib) and the others types<sup>7</sup>.

Class II c-Met inhibitors are one of the most important type, which can bind to multiple sites of c-Met kinase and are proved to be multi-target kinase inhibitors. According to the structure characteristics of Class II c-Met inhibitors, We divided the structures of Class II c-Met inhibitors into four parts A, B, C and D (**Figure 1**). The main structural modification of these inhibitors was focused on the moiety A (heterocyclic nucleus) and moiety C. The moiety C is defined as a 5-atom linker, which has two obvious structural characteristics: on the one hand, the '5 atoms regulation' means that six chemical bonds distance exists between moiety B and moiety D; on the other hand, the linker contains hydrogen, oxygen and nitrogen atoms which could provide appropriate hydrogen-bond donor or acceptor to form hydrogen bonds with amino acid residues<sup>8</sup>. Based on the above summary, taking Foretinib as lead compound, we had designed and synthesized several different series of derivatives such as compounds **6a-b**<sup>9-10</sup> and **7**<sup>11</sup> (**Figure 1**) in the past several years, which exhibited excellent anti-tumor activity and kinase activity.

According to principles of scaffold hopping and bioisosterism, various heterocyclic nucleus of c-met inhibitors had been developed, such as pyrazolo[1,5-*a*]pyridine core of compound **2**<sup>12</sup>, imidazo[1,2-*a*]pyridine core of compound **3**<sup>13</sup>, imidazo[1,2-*b*]pyridazine core of compound **4**<sup>14</sup> and imidazo[1,2-*b*]pyridazine core of compound **5**<sup>15</sup> (**Figure 1**). Among them, the activity against c-Met kinase of compounds **2**, **3** and **5** reached a single digit nanomolar level, which indicated that the modification of the heterocyclic nucleus had a critical impact on activity. It is worth mentioning that the triazole heterocyclic structure was found to be a significant group in some Class I c-Met inhibitors which exhibited excellent biological activity. Therefore, based on bioisosterism principles, the [1,2,4]triazolo[4,3-*a*]pyrazine structure was used as the core of the novel c-Met inhibitor in this research. Furthermore, in our previous study, compound **8**<sup>16</sup> showed excellent anti-tumor due to the introduction of 4-oxo-pyridazinone to the 5-atom linker moiety. So the active structure 4-oxo-pyridazinone was retained in our design (**Figure 2**). Finally, we introduced electron-withdrawing group and electron-donating group on the benzene ring to explore the effect on activity, so that the benzene ring was allowed

to occupy the internal hydrophobic pocket of c-Met and could improve the binding of the compound to the protein. Herein, based on the structure-based drug design (SBDD) strategy and bioisosterism principles, and taking Foretinib as reference compound, two series of c-Met inhibitors were designed and synthesized, culminating in the discovery of compound **22i**.

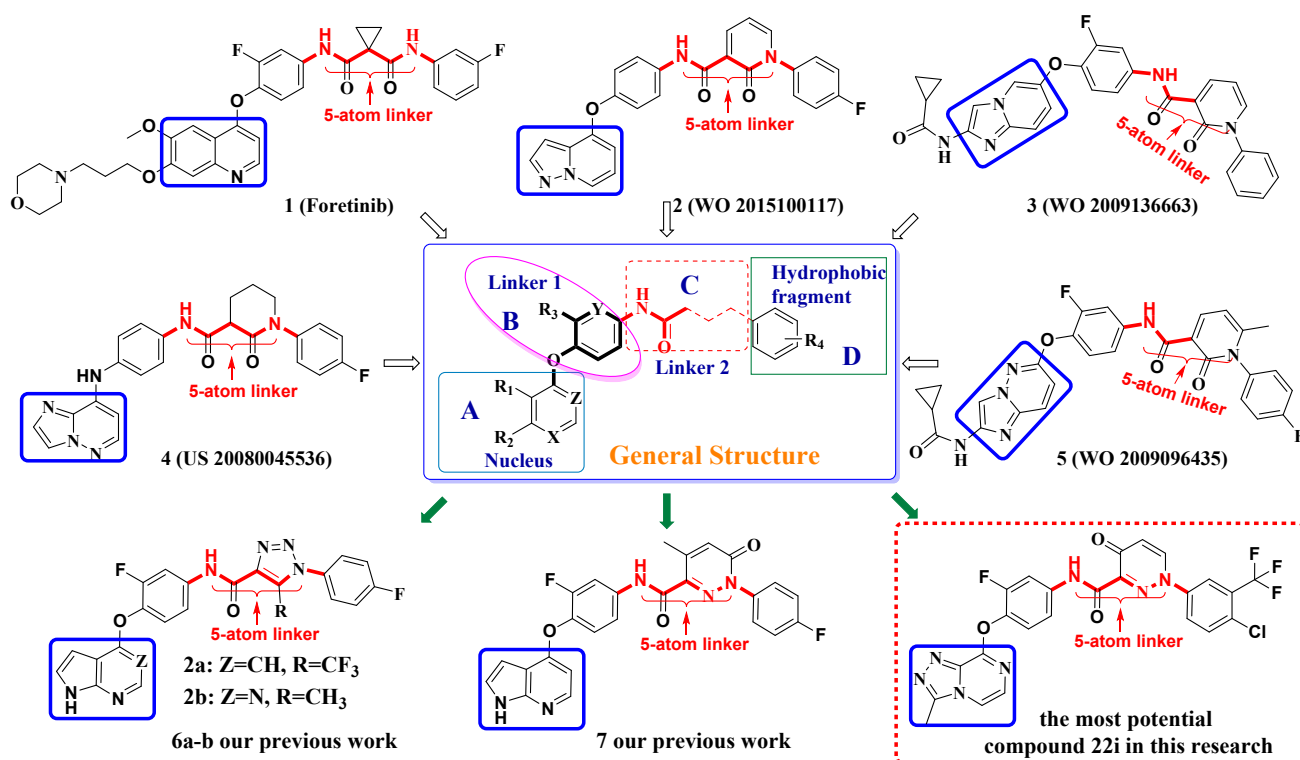


**Figure 1.** Examples of c-Met kinase inhibitors and the most potential compound **22i** in this research.

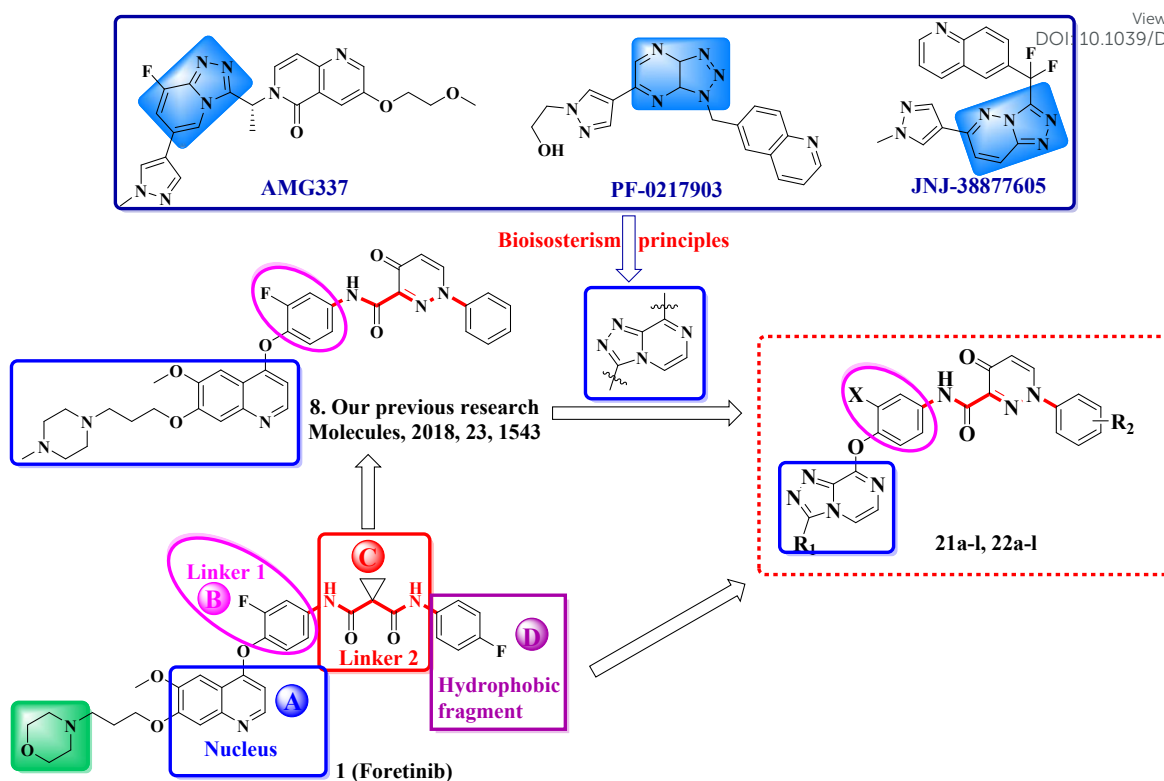


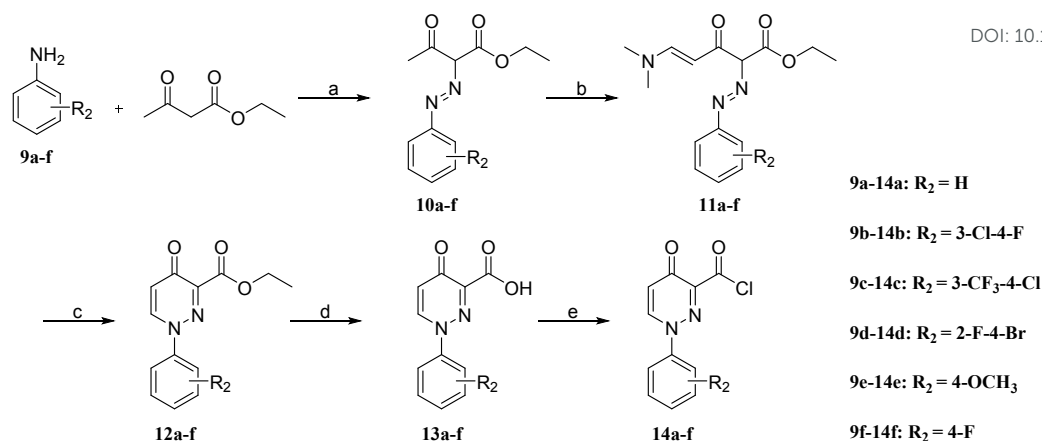
**Figure 2.** Structures and design strategy for target compounds

## 2 Results and Discussion

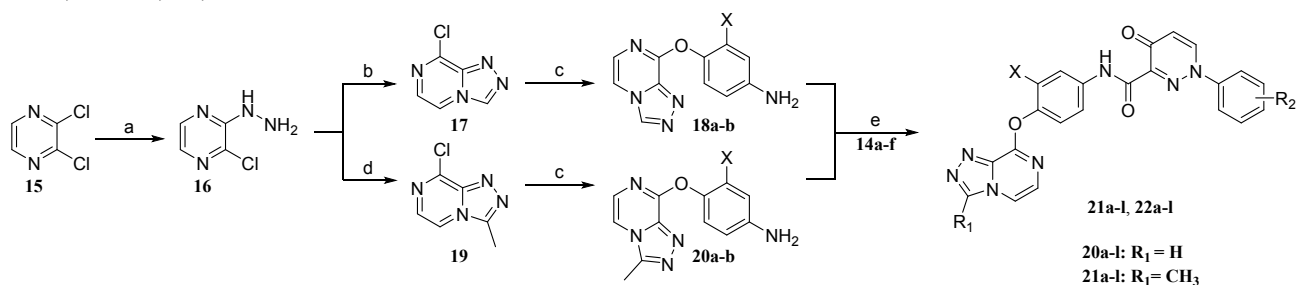
### 2.1 Chemistry

The synthetic route of intermediate compounds **14a-f** was illustrated in **Scheme 1**. Using different substituted anilines **9a-f** as starting materials, different substituted anilines **9a-f** were diazotized and then reacted with ethyl acetoacetate to obtain compounds **10a-f**. Next, compounds **10a-f** were dissolved in the DMF-DMA, heated to 100 °C and stirred for 6-10 h, and then the mixture was poured to the petroleum ether and filtered to obtain the compounds **11a-f**. Then, the cyclization was proceeded to convert **11a-f** to compounds **12a-f** in the presence of NaOH. Finally, hydrolysis and acyl chlorination were used to convert compounds **12a-f** to the key intermediate **14a-f**.

The target compounds **21a-l** and **22a-l** were prepared as outlined in **Scheme 2**. The key intermediate **17** was synthesized from 2,3-dichloropyrazine (compound **15**) *via* substitution reaction with hydrazine hydrate and cyclization with triethoxy methane, respectively. Then, compounds **18a-b** were obtained by substitution reaction with 4-aminphenol or 2-fluoro-4-aminphenol. Finally, reaction of anilines **18a-b** with acyl chloride **14a-f** promoted by DIPEA in CH<sub>2</sub>Cl<sub>2</sub> at room temperature yielded the target compounds **21a-l**<sup>9</sup>. The synthetic method of compounds **22a-l** was the same as that of the compounds **21a-l**.



**Scheme 1.** Reagents and conditions: (a) Sodium nitrite, EtOH, ethyl acetoacetate, 0 °C, 0.5 h; (b) DMF-DMA, 100 °C, reflux, 6-10 h; (c) EtOH, 10% NaOH, 80 °C, 1 h; (d) Sodium carbonate, EtOH/H<sub>2</sub>O, 80 °C, 3-5 h; (e) Oxalyl chloride, DMF, CH<sub>2</sub>Cl<sub>2</sub>, r.t., 5 min.



**Scheme 2.** Reagents and conditions: (a) N<sub>2</sub>H<sub>4</sub>·H<sub>2</sub>O, EtOH, 85 °C, reflux; (b) Triethoxy methane, 80 °C, reflux; (c) 4-Aminophenol, potassium *t*-butoxide, KI, THF; (d) Triethyl orthoacetate, 80 °C, reflux; (n) DIPEA, CH<sub>2</sub>Cl<sub>2</sub>, r.t., 0.5 h.

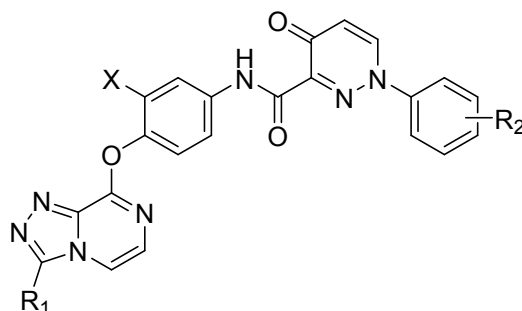
## 2.2 Biological Evaluation

Three cancer cell lines A549, MCF-7 and Hela were selected for evaluating the anti-tumor activities of the target compounds by the method of MTT (3-(4,5-dimethylthiazolyl-2)-2,5-diphenyltetrazolium bromide), and the results were shown in **Table 1**. As can be seen, most of the target compounds showed moderate to excellent levels of anti-tumor activity *in vitro* against three tested cell lines. In addition, most of the compounds had more potent anti-tumor activities against both A549 and Hela cell lines than against MCF-7 cell line. Among them, compound **22i** exhibited excellent anti-tumor potency for A549, MCF-7 and Hela cell lines with IC<sub>50</sub> values of 0.83 ± 0.07 μM, 0.15 ± 0.08 μM and 2.85 ± 0.74 μM, respectively.

Further investigations about the effects of different substituents on the benzene ring were carried out, which revealed that the electron-withdrawing group on the benzene ring could increase the *in vitro* anti-tumor activity of the target compounds, and the opposite was true. For example, the compounds **21e**, **21k**, **22e** and **22k** with methoxy group showed lower *in vitro* anti-tumor activities than that of the target compounds with electron-withdrawing group. The target compounds bearing a larger substituent (trifluoromethyl group) on the phenyl ring exhibited better anti-tumor activity such as compound **21i** (R<sub>2</sub>=3-CF<sub>3</sub>-4-Cl) and **22i** (R<sub>2</sub>=3-CF<sub>3</sub>-4-Cl). Furthermore, in order to investigate the

cytotoxic activity of the target compounds on normal cells, the *in vitro* cytotoxic activity against LO2 normal liver cell line was carried out. The results presenting in **Table 1** indicated that the 24 target compounds had little cytotoxic activity against LO2 normal liver cell line, and their IC<sub>50</sub> values were greater than 50 μM. These data indicated that the three cancer cell lines (A549, MCF-7 and Hela) were more sensitive to the target compounds than LO2 normal liver cell line.

**Table 1**  
c-Met inhibitory activities and anti-tumor activities of target compounds.



Compounds	X	R <sub>1</sub>	R <sub>2</sub>	IC <sub>50</sub> (μM) <sup>a</sup>				
				A549	MCF-7	Hela	LO2	c-Met
21a	H	H	H	5.21 ± 0.48	4.78 ± 0.52	10.58 ± 0.85	>50	0.238
21b	H	H	3-Cl-4-F	15.73 ± 1.27	20.69 ± 1.61	26.45 ± 2.13	>50	>1
21c	H	H	3-CF <sub>3</sub> -4-Cl	13.74 ± 1.48	19.01 ± 1.77	25.01 ± 1.93	>50	>1
21d	H	H	2-F-4-Br	17.48 ± 1.57	22.17 ± 0.38	28.25 ± 0.85	>50	>1
21e	H	H	4-OCH <sub>3</sub>	23.62 ± 1.15	34.73 ± 1.92	>50	>50	>1
21f	H	H	4-F	2.48 ± 0.35	3.18 ± 0.42	6.68 ± 0.56	>50	0.095
21g	F	H	H	13.48 ± 0.67	16.95 ± 1.81	23.26 ± 1.53	>50	>1
21h	F	H	3-Cl-4-F	4.25 ± 0.62	3.09 ± 0.30	8.89 ± 0.96	>50	0.120
21i	F	H	3-CF <sub>3</sub> -4-Cl	0.89 ± 0.07	1.64 ± 0.56	2.56 ± 0.49	>50	0.055
21j	F	H	2-F-4-Br	5.15 ± 0.51	6.13 ± 0.58	11.87 ± 1.29	>50	0.280
21k	F	H	4-OCH <sub>3</sub>	14.56 ± 1.04	27.42 ± 2.24	>50	>50	ND <sup>b</sup>
21l	F	H	4-F	4.87 ± 0.19	4.45 ± 0.32	8.36 ± 0.54	>50	0.126
22a	H	CH <sub>3</sub>	H	13.16 ± 0.77	15.90 ± 1.25	19.27 ± 1.48	>50	0.768
22b	H	CH <sub>3</sub>	3-Cl-4-F	12.67 ± 0.92	16.48 ± 1.69	20.74 ± 1.24	>50	>1
22c	H	CH <sub>3</sub>	3-CF <sub>3</sub> -4-Cl	7.82 ± 0.75	8.77 ± 0.86	13.58 ± 0.92	>50	0.440
22d	H	CH <sub>3</sub>	2-F-4-Br	28.25 ± 1.57	30.48 ± 1.63	35.62 ± 1.78	>50	ND
22e	H	CH <sub>3</sub>	4-OCH <sub>3</sub>	13.23 ± 1.42	16.09 ± 1.59	29.32 ± 2.17	>50	0.880
22f	H	CH <sub>3</sub>	4-F	18.31 ± 1.64	19.85 ± 1.94	33.27 ± 2.31	>50	>1
22g	F	CH <sub>3</sub>	H	2.04 ± 0.25	2.16 ± 0.39	4.42 ± 0.65	>50	0.089

<b>22h</b>	F	CH <sub>3</sub>	3-Cl-4-F	6.72 ± 0.85	6.49 ± 0.79	12.54 ± 0.98	>50	0.300	0.300
<b>22i</b>	F	CH <sub>3</sub>	3-CF <sub>3</sub> -4-Cl	0.83 ± 0.07	0.15 ± 0.08	2.85 ± 0.74	>50	0.048	0.048
<b>22j</b>	F	CH <sub>3</sub>	2-F-4-Br	23.42 ± 0.75	16.48 ± 0.57	24.26 ± 1.87	>50	ND	ND
<b>22k</b>	F	CH <sub>3</sub>	4-OCH <sub>3</sub>	11.56 ± 0.42	16.79 ± 1.27	25.38 ± 1.25	>50	>1	>1
<b>22l</b>	F	CH <sub>3</sub>	4-F	5.65 ± 0.20	6.42 ± 0.34	8.05 ± 0.31	>50	ND	ND
Foretinib <sup>c</sup>	-	-	-	0.71 ± 0.05	0.93 ± 0.09	-	ND	ND	0.019

<sup>a</sup> The values are an average of two separate determinations.

<sup>b</sup> ND: Not detected.

<sup>c</sup> Used as a positive control.

Through homogeneous time-resolved fluorescence (HTRF<sup>®</sup>) assays, experiments against c-Met kinase of twenty selected target compounds as well as the reference compound Foretinib were carried out for further study. The obtained results were presented in **Table 1**, which suggested that most of the target compounds exhibited moderate inhibition activity on c-Met kinase. The results indicated that the target compounds may act through inhibiting the c-Met signal pathway. Furthermore, the c-Met kinase activity of target compounds **21f** (0.095 μM), **21i** (0.055 μM), **22g** (0.089 μM) and **22i** (0.048 μM) at nanomolar level were slightly lower than that of the reference Foretinib (0.019 μM). The anti-tumor activity and c-met kinase activity of compound **22i** were slightly better than that of compound **21i**, which may be due to the introduction of a methyl group into the nucleus of compound **22i** which were advanced for sufficiently occupied the cavity of c-Met protein.

In addition, the most promising compound **22i** was selected as a representative to evaluate the relationship between the anti-tumor activity and the concentration of the target compounds by the method of MTT. Three cancer cell lines A549, MCF-7 and Hela were treated with seven different concentrations of compound **22i** for 72 h, respectively, and the results were shown in **Figure 3**. As can be seen, as the concentration of compound **22i** increasing, the inhibition rate of compound **22i** on the three cancer cell lines increased, and the phenomenon of dose-dependent was observed. Furthermore, we can find that compound **22i** had better anti-tumor activity against MCF-7 and A549 than against Hela.

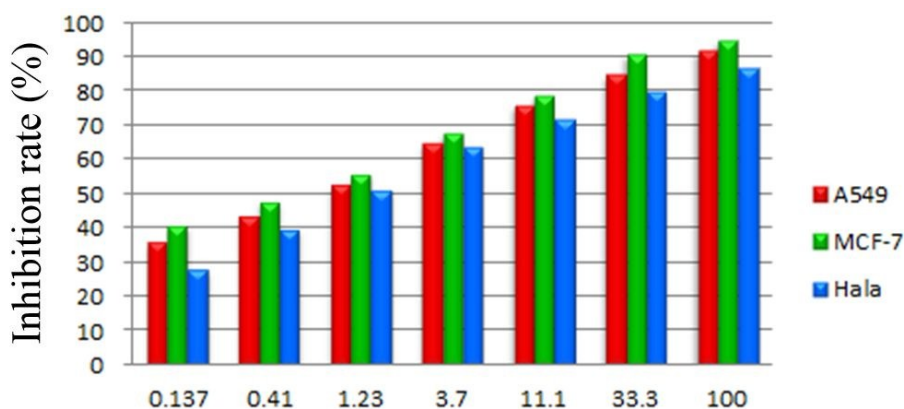


**Figure 3.** Relationship between activity and concentration of compound **22i** against three cancer cell lines.

### 2.3 Effect on cell cycle progression.

View Article Online  
DOI: 10.1039/D0NJ00575D

In order to have a deeper understanding of the growth inhibition mechanism of target compounds to cancer cells, the effect of compound **22i** on cell cycle progression was investigated. A549 cells were treated with 1.0  $\mu\text{M}$  of compound **22i** for 72 h, and then the flow cytometric cycle experiment was carried out. Compared with the control group, the population of G0/G1 phase increased significantly after treatment of A549 with compound **22i**, increasing from 60.54% to 73.86%, while the S phase decreased correspondingly, and there was no significant change in G2/M phase. It indicated that compound **22i** could induce cell cycle arrest of A549 cells at the G0/G1 checkpoint.

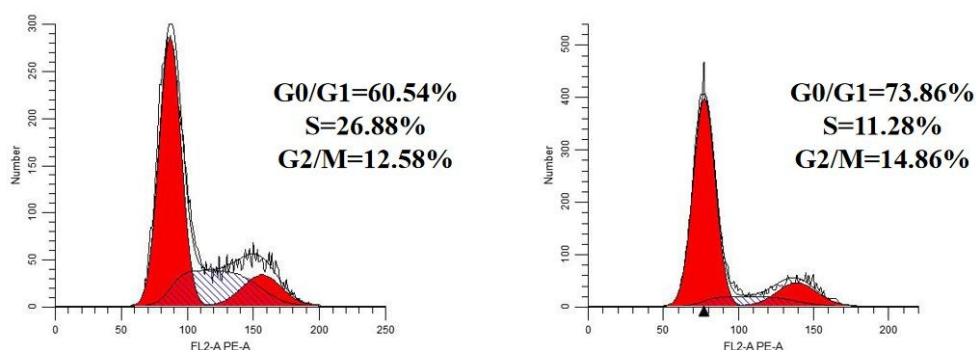


**Figure 4.** Cell cycle progression analyses of A549 cells treated with compound **22i** for 72 h.

### 2.4 Apoptosis result analyzing

To further explain the inhibitory effect of compound **22i** on cancer cell growth, the apoptosis-inducing effect of compound **22i** on A549 cells was evaluated by flow cytometry. As can be seen from the **Figure 5**, compound **22i** significantly induced early apoptosis and late apoptosis in A549 cells, especially late apoptosis, reaching 9.16% at the concentration of 1.00  $\mu\text{M}$ . As the concentration of compound **22i** increasing, the total apoptosis rate was also increased, from 6.43% to 15.87% in a dose-dependent manner. These data demonstrated that compound **22i** could induced apoptosis in A549 cells in a dose-dependent manner.

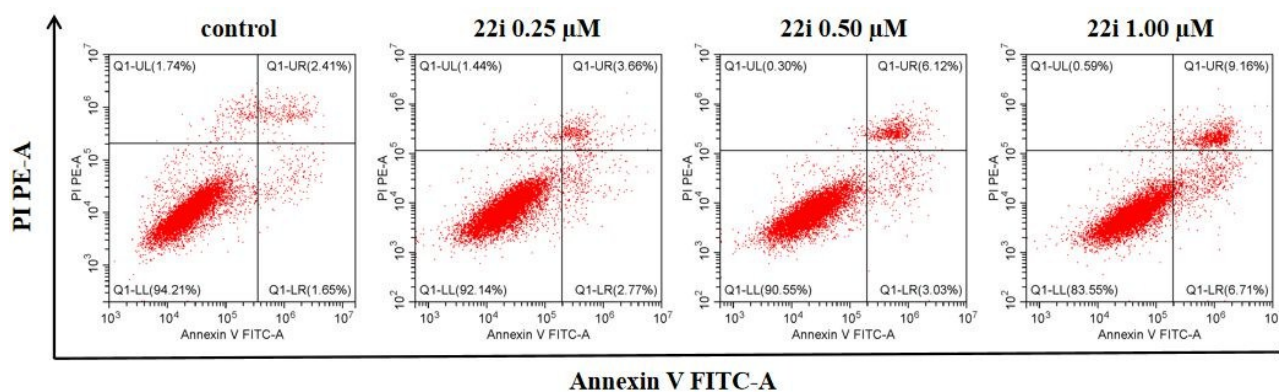


**Figure 5.** Apoptosis analyses of A549 cells treated with compound **22i** for 72 h.

### 2.5 Morphologic changes of A549 cells under inverted microscopy and fluorescence microscopy

To further verify that compound **22i** can induce apoptosis in A549 cells, morphological changes of A549 cells treated with compound **22i** for 12 h were observed by AO fluorescence staining. As illustrated in **Figure 6A**, A549 cells in the control group grew well, the cells were full and the edges were clear. However, when A549 cells were treated with 0.83  $\mu$ M of compound **22i** for 12 h, the obtained result was presented in **Figure 6B**, in which the A549 cells shrank, the chromatin was condensed and the nucleus was orange. The results further indicated that compound **22i** successfully induced apoptosis in A549 cells.

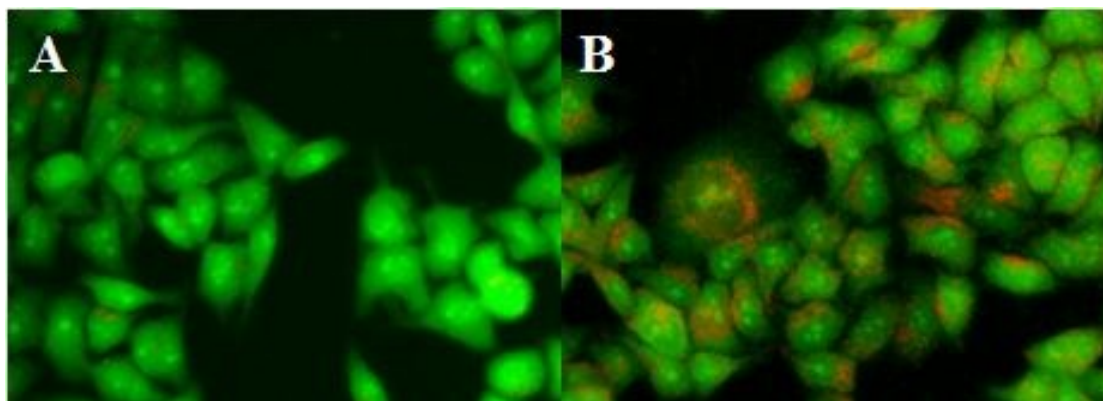


**Figure 6.** Observation of A549 cells morphology by AO fluorescence staining

## 2.6 Molecular docking study

According to the results of *in vitro* anti-tumor activity assays and enzymatic activity assay, we selected compound **22i** as the representative to dock with c-Met protein (PDB code 3LQ8) by AutoDock 4.2 software (The Scripps Research Institute, USA), and the docking results were processed and modified in PyMOL 1.8.x software (<https://pymol.org>). As illustrated in **Figure 7a**, the whole compound **22i** skeleton embedded into hydrophobic pocket of c-Met protein and closely combined with c-Met protein. As can be seen from **Figure 7b**, the two nitrogen atoms on the triazolopyrazine core structure can form a bidentate hydrogen bond with the key amino acid residue MET1160 in the hinge region, demonstrating that the introduction of the triazolopyrazine core ensured the activity of the target compounds. In the 5-atom linker, the oxygen atom of the pyridazinone group formed a hydrogen bond with LYS1110, and the two nitrogen atoms on the pyridazinone group formed a bidentate hydrogen bond with residue ASP1222. The molecular docking studies suggested that compound **22i** may be a potential inhibitor of c-Met.

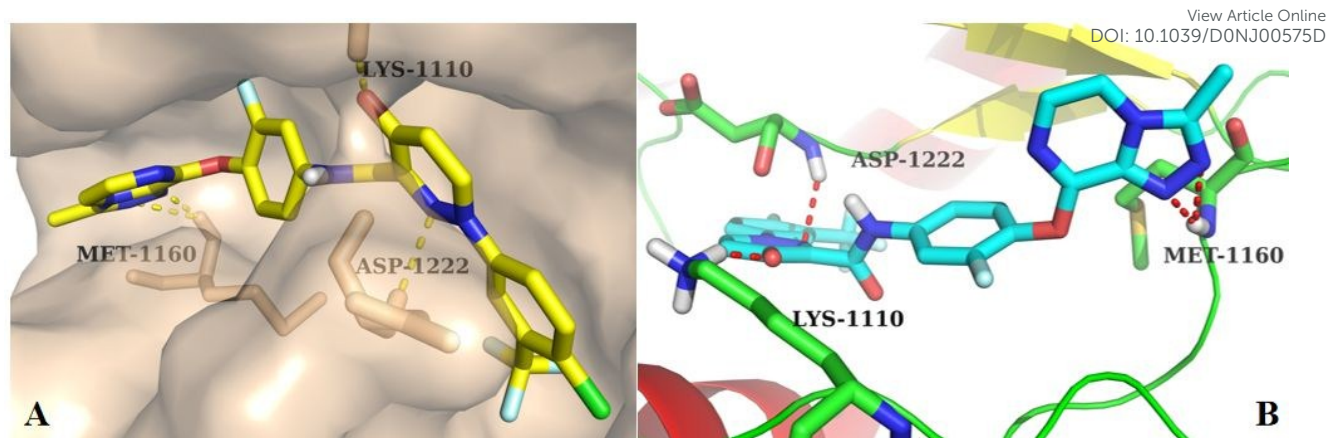


**Figure 7.** The docking mode of compound **22i** with c-Met (PDB code 3LQ8)

### 3 Experimental Section

#### 3.1 General Information

All melting points were obtained on a Büchi Melting Point B-540 apparatus (Büchi Labortechnik, Flawil, Switzerland) and were uncorrected. Frequently used solvents (Methanol, DCM, EA, DMF, etc.) were absolutely anhydrous. TLC analysis was carried out on silica gel plates GF254 (Qindao Haiyang Chemical, China) with fluorescent indicator 254 nm. Column chromatography was run on silica gel (200-300 mesh) from Qingdao Ocean Chemicals (Qingdao, Shandong, China). Mass spectrometry (MS) was performed on Waters High Resolution Quadrupole Time of Flight Tandem Mass Spectrometry (QTOF). The purity of the compound was determined by Agilent 1260 liquid chromatograph fitted with an Inertex-C18 column. <sup>1</sup>HNMR and <sup>13</sup>CNMR spectra were recorded on Bruker ARX-400, 400 MHz spectrometers (Bruker Bioscience, Billerica, MA, USA) with tetramethylsilane (TMS) as an internal standard.

#### 3.2 Chemistry

##### 3.2.1 Preparation of intermediate compounds **14a-f**

The preparation of intermediate compounds **14a-f** had been described in detail in our previous work <sup>17</sup>.

##### 3.2.2 Preparation of compound **16**

2,3-Dichloropyrazine (20 g, 0.134 mol) was dissolved in ethanol, and a small amount of hydrazine hydrate (21 g, 0.42 mol) was added thereto in multiple portions. The mixture was refluxed at 80 °C and monitored by TLC. After the reaction mixture was cooled, it was added to ice water, and then the precipitated solid was filtered and dried to give compound **16** (16.8 g, 84.1%) as yellow powder.

##### 3.2.3 Preparation of compound **17**

Intermediate compound **16** (5.0 g, 0.034 mol) was added to triethyl orthoformate (50 mL) for 2 h at 80 °C. The

reaction solution was directly filtered under suction, and the filter cake was washed with petroleum ether and dried to yield compound **17** (4.8 g, yield 90.1%) as yellow powder.

#### 3.2.4 Preparation of compounds **18a-b**

4-aminophenol and potassium t-butoxide (1.46 g, 13.0 mmol) were added to tetrahydrofuran, and the mixture was stirred for 1 h at 0 °C. Intermediate **18** (1.00 g, 6.5 mmol) and potassium iodide (0.12 g, 0.72 mmol) were added to the flask in which tetrahydrofuran was used as a solvent, then the mixture was heated to 80 °C, and the above-mentioned 4-aminophenol was added there under nitrogen atmosphere. After the reaction was completed, the mixture was filtered, and the filtrate was evaporated to dryness. After evaporation, a small amount of NaOH aqueous solution was added to the mixture, and a solid was precipitated, filtered, and dried to give compound **18a** (0.45 g, 30.6%) as grayish white solid. The preparation method of compound **18b** was the same as that of the compound **18a**.

#### 3.2.5 Preparation of compound **19**

The preparation method of compound **19** was the same as that of the compound **17**.

#### 3.2.6 Preparation of compounds **20a-b**

The preparation method of compounds **20a-b** were the same as that of the compound **18a**.

#### 3.2.7 Preparation of compounds **21a-l**

Compounds **14a-f** (0.51 mmol) and N,N-diisopropylethylamine (0.49 mmol) were dissolved in dichloromethane (10 mL), and then compounds **18a-b** were added dropwise under ice bath. Then, the reaction mixture was taken from ice bath, stirred at room temperature for 0.5 h. The reaction was washed with 10% aqueous K<sub>2</sub>CO<sub>3</sub> (50 mL), and the organic layer was dried over anhydrous Na<sub>2</sub>SO<sub>4</sub> and concentrated in reduced pressure to obtain the crude product. The crude product was purified through a column chromatography on silica to yield compounds **21a-l**.

#### 3.2.8 Preparation of compounds **22a-l**

The preparation method of compounds **22a-l** were the same as that of the compounds **21a-l**.

*N*-(4-([1,2,4]triazolo[4,3-*a*]pyrazin-8-yloxy)phenyl)-4-oxo-1-phenyl-1,4-dihydropyridazine-3-carboxamide (**21a**).

Light yellow solid in 31.2% yield. m.p: 304.4–306.1 °C. <sup>1</sup>H NMR (400 MHz, DMSO-*d*<sub>6</sub>) δ 11.80 (s, 1H), 9.34 (s, 1H), 8.89 (d, *J* = 7.7 Hz, 1H), 8.18 (d, *J* = 4.4 Hz, 1H), 7.69 (d, *J* = 8.1 Hz, 4H), 7.49 (t, *J* = 7.6 Hz, 2H), 7.40 (d, *J* = 7.4 Hz, 1H), 7.24 (t, *J* = 6.0 Hz, 3H), 6.80 (d, *J* = 7.6 Hz, 1H). <sup>13</sup>C NMR (101 MHz, DMSO-*d*<sub>6</sub>) δ 169.74, 160.48, 152.01, 147.06, 143.39, 142.31, 139.61, 130.22 (2C), 129.95, 129.14, 127.47, 126.01, 125.13, 121.89 (2C), 120.78, 119.33, 116.78, 116.09, 114.62, 108.88. IR (KBr) cm<sup>-1</sup>: 3442, 3038, 1688, 1596, 1565, 1492, 1330, 1205. TOF MS ES+ (*m/z*): [M + H]<sup>+</sup>, calcd for C<sub>22</sub>H<sub>15</sub>N<sub>7</sub>O<sub>3</sub>: 426.1315, found, 426.1316. HPLC purity: 97.22% (Column: Dikma Luna C18; Mobile

phase: H<sub>2</sub>O:MeCN = 70:30; Column temperature: 26 °C; Wavelength: 280 nm; Flow rate: 1.0 mL/min) DOI: 10.1039/D0NJ00575D

View Article Online

***N-(4-([1,2,4]triazolo[4,3-a]pyrazin-8-yloxy)phenyl)-1-(3-chloro-4-fluorophenyl)-4-oxo-1,4-dihydropyridazine-3-carboxamide (21b).***

Brown solid in 51.2% yield. m.p: 248.0–251.3 °C. <sup>1</sup>H NMR (400 MHz, DMSO-*d*<sub>6</sub>) δ 11.74 (s, 1H), 9.35 (s, 1H), 8.91–8.82 (m, 1H), 8.20 (d, *J* = 4.5 Hz, 1H), 8.02 (t, *J* = 4.5 Hz, 1H), 7.72 (d, *J* = 8.7 Hz, 3H), 7.57 (s, 1H), 7.29 (d, *J* = 9.1 Hz, 3H), 6.82 (d, *J* = 7.9 Hz, 1H). <sup>13</sup>C NMR (101 MHz, DMSO-*d*<sub>6</sub>) δ 169.72, 160.47, 151.88, 147.93, 143.36, 142.35, 139.35, 138.61, 137.77, 135.00, 130.22 (2C), 129.14, 126.53 (2C), 125.18, 121.89 (2C), 121.08, 116.73, 115.78, 108.81. IR (KBr) cm<sup>-1</sup>: 3441, 3044, 1688, 1601, 1559, 1490, 1326, 1200. TOF MS ES+ (*m/z*): [M + H]<sup>+</sup>, calcd for C<sub>22</sub>H<sub>13</sub>ClFN<sub>7</sub>O<sub>3</sub>: 478.0831, found, 478.0830. HPLC purity: 97.51% (Column: Dikma Luna C18; Mobile phase: H<sub>2</sub>O:MeCN = 60:40; Column temperature: 26 °C; Wavelength: 280 nm; Flow rate: 1.0 mL/min).

***N-(4-([1,2,4]triazolo[4,3-a]pyrazin-8-yloxy)phenyl)-1-(4-chloro-3-(trifluoromethyl)phenyl)-4-oxo-1,4-dihydropyridazine-3-carboxamide (21c).***

Grayish white solid in 61.2% yield. m.p: 283.5–284.9 °C. <sup>1</sup>H NMR (400 MHz, DMSO-*d*<sub>6</sub>) δ 11.71 (s, 1H), 9.39 (s, 1H), 9.03 (d, *J* = 7.9 Hz, 1H), 8.23 (d, *J* = 5.2 Hz, 2H), 8.09 (d, *J* = 8.9 Hz, 1H), 7.92 (d, *J* = 8.9 Hz, 1H), 7.74 (d, *J* = 8.3 Hz, 2H), 7.30 (d, *J* = 8.6 Hz, 3H), 6.86 (d, *J* = 7.7 Hz, 1H). <sup>13</sup>C NMR (101 MHz, DMSO-*d*<sub>6</sub>) δ 169.91, 159.91, 153.10, 148.42, 142.23, 142.20, 139.14 (2C), 136.30, 133.55 (2C), 130.83, 128.28, 127.96, 127.23, 126.75, 124.17, 123.00 (2C), 121.50 (2C), 120.65, 115.10. IR (KBr) cm<sup>-1</sup>: 3077, 1687, 1599, 1560, 1488, 1326, 1201. TOF MS ES+ (*m/z*): [M + H]<sup>+</sup>, calcd for C<sub>23</sub>H<sub>13</sub>ClF<sub>3</sub>N<sub>7</sub>O<sub>3</sub>: 528.0799, found, 528.0799. HPLC purity: 96.91% (Column: Dikma Luna C18; Mobile phase: H<sub>2</sub>O:MeCN = 50:50; Column temperature: 26 °C; Wavelength: 280 nm; Flow rate: 1.0 mL/min).

***N-(4-([1,2,4]triazolo[4,3-a]pyrazin-8-yloxy)phenyl)-1-(4-bromo-2-fluorophenyl)-4-oxo-1,4-dihydropyridazine-3-carboxamide (21d).***

White solid in 31.2% yield. m.p: 286.3–298.5 °C. <sup>1</sup>H NMR (400 MHz, DMSO-*d*<sub>6</sub>) δ 11.60 (s, 1H), 9.38 (s, 1H), 8.65 (s, 1H), 8.23 (d, *J* = 4.2 Hz, 1H), 7.85 (d, *J* = 10.2 Hz, 1H), 7.71 (d, *J* = 8.8 Hz, 3H), 7.62 (s, 1H), 7.28 (s, 3H), 6.81 (d, *J* = 8.4 Hz, 1H). <sup>13</sup>C NMR (101 MHz, DMSO-*d*<sub>6</sub>) δ 169.45, 159.93, 153.10, 148.36, 144.98, 139.15 (2C), 136.29, 130.95, 129.20, 129.14 (2C), 126.75, 123.45, 123.02 (2C), 121.46 (2C), 121.10, 120.87, 120.13, 115.10. IR (KBr) cm<sup>-1</sup>: 3441, 3074, 1689, 1607, 1569, 1484, 1322, 1202. TOF MS ES+ (*m/z*): [M + H]<sup>+</sup>, calcd for C<sub>22</sub>H<sub>13</sub>BrFN<sub>7</sub>O<sub>3</sub>: 522.0326, found, 522.0327. HPLC purity: 96.22% (Column: Dikma Luna C18; Mobile phase: H<sub>2</sub>O:MeCN = 60:40; Column temperature: 26 °C; Wavelength: 280 nm; Flow rate: 1.0 mL/min).

***N-(4-([1,2,4]triazolo[4,3-a]pyrazin-8-yloxy)phenyl)-1-(4-methoxyphenyl)-4-oxo-1,4-dihydropyridazine-3-carboxamide (21e).***

Brown solid in 20.2% yield. m.p: 293.5–295.7 °C. <sup>1</sup>H NMR (400 MHz, DMSO-*d*<sub>6</sub>) δ 11.97 (s, 1H), 9.39 (s, 1H),

8.84 (s, 1H), 8.23 (s, 1H), 7.70 (d,  $J = 37.9$  Hz, 3H), 7.44 (s, 1H), 7.30 (s, 2H), 7.08 (s, 2H), 6.84 (s, 2H), 6.77 (s, 3H).  $^{13}\text{C}$  NMR (101 MHz, DMSO- $d_6$ )  $\delta$  170.45, 160.82, 153.82, 148.28, 143.12, 142.04, 139.84 (2C), 137.66, 137.10, 127.46, 124.25 (2C), 123.73 (2C), 122.16, 121.80, 120.61, 120.56, 115.90 (2C), 115.78, 56.89. IR (KBr)  $\text{cm}^{-1}$ : 3443, 3104, 1688, 1597, 1567, 1507, 1332, 1202. TOF MS ES+ ( $m/z$ ):  $[\text{M} + \text{H}]^+$ , calcd for  $\text{C}_{23}\text{H}_{17}\text{N}_7\text{O}_4$ : 456.1420, found, 456.1417. HPLC purity: 98.93% (Column: Dikma Luna C18; Mobile phase:  $\text{H}_2\text{O}:\text{MeCN} = 70:30$ ; Column temperature: 26 °C; Wavelength: 280 nm; Flow rate: 1.0 mL/min).

***N-(4-([1,2,4]triazolo[4,3-*a*]pyrazin-8-yloxy)phenyl)-1-(4-fluorophenyl)-4-oxo-1,4-dihydropyridazine-3-carboxamide (21f).***

Yellow solid in 41.3% yield. m.p: 309.4–311.7 °C.  $^1\text{H}$  NMR (400 MHz, DMSO- $d_6$ )  $\delta$  11.81 (s, 1H), 9.37 (s, 1H), 8.88 (s, 1H), 8.23 (s, 1H), 7.77 (d,  $J = 17.4$  Hz, 4H), 7.39 (s, 2H), 7.29 (s, 3H), 6.84 (s, 1H).  $^{13}\text{C}$  NMR (101 MHz, DMSO- $d_6$ )  $\delta$  171.82, 160.23, 153.12, 148.04, 145.97, 140.90, 139.13 (2C), 136.35, 130.14, 126.75, 124.47, 124.38, 123.03 (2C), 121.46 (2C), 120.89, 117.10 (2C), 116.87, 115.09. IR (KBr)  $\text{cm}^{-1}$ : 3444, 3107, 1688, 1598, 1564, 1508, 1328, 1204. TOF MS ES+ ( $m/z$ ):  $[\text{M} + \text{H}]^+$ , calcd for  $\text{C}_{22}\text{H}_{14}\text{FN}_7\text{O}_3$ : 444.1220, found, 444.1223. HPLC purity: 96.51% (Column: Dikma Luna C18; Mobile phase:  $\text{H}_2\text{O}:\text{MeCN} = 70:30$ ; Column temperature: 26 °C; Wavelength: 280 nm; Flow rate: 1.0 mL/min).

***N-(4-([1,2,4]triazolo[4,3-*a*]pyrazin-8-yloxy)-3-fluorophenyl)-4-oxo-1-phenyl-1,4-dihydropyridazine-3-carboxamide (21g).***

White solid in 28.2% yield. m.p: 296.3–298.5 °C.  $^1\text{H}$  NMR (400 MHz, DMSO- $d_6$ )  $\delta$  11.97 (s, 1H), 9.42 (s, 1H), 8.94 (d,  $J = 7.9$  Hz, 1H), 8.33–8.25 (m, 1H), 7.89 (d,  $J = 12.5$  Hz, 1H), 7.74 (d,  $J = 7.8$  Hz, 2H), 7.55 (t,  $J = 7.8$  Hz, 2H), 7.45 (s, 3H), 7.32 (s, 1H), 6.86 (d,  $J = 7.8$  Hz, 1H).  $^{13}\text{C}$  NMR (101 MHz, DMSO- $d_6$ )  $\delta$  170.55, 160.84, 153.88, 149.11, 148.88, 147.48, 142.95 (2C), 140.18, 130.83 (2C), 129.92, 129.80, 126.97, 123.68 (2C), 122.71, 122.60 (2C), 122.17, 121.67, 114.63. IR (KBr)  $\text{cm}^{-1}$ : 3446, 3108, 1699, 1591, 1563, 1490, 1327, 1205. TOF MS ES+ ( $m/z$ ):  $[\text{M} + \text{H}]^+$ , calcd for  $\text{C}_{22}\text{H}_{14}\text{FN}_7\text{O}_3$ : 444.1220, found, 444.1219. HPLC purity: 98.20% (Column: Dikma Luna C18; Mobile phase:  $\text{H}_2\text{O}:\text{MeCN} = 70:30$ ; Column temperature: 26 °C; Wavelength: 280 nm; Flow rate: 1.0 mL/min).

***N-(4-([1,2,4]triazolo[4,3-*a*]pyrazin-8-yloxy)-3-fluorophenyl)-1-(3-chloro-4-fluorophenyl)-4-oxo-1,4-dihydropyridazine-3-carboxamide (21h).***

Light yellow solid in 36.5% yield. m.p: 273.1–275.6 °C.  $^1\text{H}$  NMR (400 MHz, DMSO- $d_6$ )  $\delta$  11.86 (s, 1H), 9.42 (s, 1H), 8.93 (d,  $J = 8.2$  Hz, 1H), 8.29 (s, 1H), 8.06 (s, 1H), 7.88 (d,  $J = 12.2$  Hz, 1H), 7.78 (d,  $J = 6.4$  Hz, 1H), 7.62 (t,  $J = 9.1$  Hz, 1H), 7.45 (s, 2H), 7.31 (s, 1H), 6.86 (d,  $J = 7.8$  Hz, 1H).  $^{13}\text{C}$  NMR (101 MHz, DMSO- $d_6$ )  $\delta$  169.68, 160.28, 148.03, 142.46, 140.24, 139.34, 138.64, 128.87, 126.53 (2C), 125.17 (2C), 124.38 (2C), 122.84, 120.84 (2C), 118.45,

118.22, 116.80, 115.78, 108.67. IR (KBr)  $\text{cm}^{-1}$ : 3445, 3095, 1703, 1604, 1562, 1495, 1333, 1212. TOF MS ES+ ( $m/z$ ): [M + H]<sup>+</sup>, calcd for C<sub>22</sub>H<sub>12</sub>ClF<sub>2</sub>N<sub>7</sub>O<sub>3</sub>: 496.0736, found, 496.0736. HPLC purity: 97.25% (Column: Dikma Luna C18; Mobile phase: H<sub>2</sub>O:MeCN = 50:50; Column temperature: 26 °C; Wavelength: 280 nm; Flow rate: 1.0 mL/min).

View Article Online  
DOI: 10.15025/NJC.2015.00575D

[M + H]<sup>+</sup>, calcd for C<sub>22</sub>H<sub>12</sub>ClF<sub>2</sub>N<sub>7</sub>O<sub>3</sub>: 496.0736, found, 496.0736. HPLC purity: 97.25% (Column: Dikma Luna C18; Mobile phase: H<sub>2</sub>O:MeCN = 50:50; Column temperature: 26 °C; Wavelength: 280 nm; Flow rate: 1.0 mL/min).

***N*-(4-([1,2,4]triazolo[4,3-*a*]pyrazin-8-yl)oxy)-3-fluorophenyl)-1-(4-chloro-3-(trifluoromethyl)phenyl)-4-oxo-1,4-dihydropyridazine-3-carboxamide (21i).**

Brown solid in 43.2% yield. m.p: 239.4–241.7 °C. <sup>1</sup>H NMR (400 MHz, DMSO-*d*<sub>6</sub>)  $\delta$  11.83 (s, 1H), 9.42 (s, 1H), 9.03 (d, *J* = 7.8 Hz, 1H), 8.29 (d, *J* = 4.7 Hz, 1H), 8.22 (s, 1H), 8.09 (d, *J* = 7.9 Hz, 1H), 7.93–7.86 (m, 2H), 7.45 (s, 2H), 7.31 (d, *J* = 4.5 Hz, 1H), 6.86 (d, *J* = 7.8 Hz, 1H). <sup>13</sup>C NMR (101 MHz, DMSO-*d*<sub>6</sub>)  $\delta$  169.01, 159.56, 151.18, 147.65, 141.61, 141.43, 138.63, 137.92, 136.92, 132.83 (2C), 130.14, 126.54, 125.82 (2C), 124.43, 120.74, 120.01 (2C), 116.08, 115.08 (2C), 108.18. IR (KBr)  $\text{cm}^{-1}$ : 3444, 3036, 1703, 1611, 1558, 1505, 1327, 1189. TOF MS ES+ ( $m/z$ ): [M + H]<sup>+</sup>, calcd for C<sub>23</sub>H<sub>12</sub>ClF<sub>4</sub>N<sub>7</sub>O<sub>3</sub>: 546.0705, found, 546.0706. HPLC purity: 96.48% (Column: Dikma Luna C18; Mobile phase: H<sub>2</sub>O:MeCN = 50:50; Column temperature: 26 °C; Wavelength: 280 nm; Flow rate: 1.0 mL/min).

***N*-(4-([1,2,4]triazolo[4,3-*a*]pyrazin-8-yl)oxy)-3-fluorophenyl)-1-(4-bromo-2-fluorophenyl)-4-oxo-1,4-dihydropyridazine-3-carboxamide (21j).**

Brown solid in 28.2% yield. m.p: 289.3–292.2 °C. <sup>1</sup>H NMR (400 MHz, DMSO-*d*<sub>6</sub>)  $\delta$  11.76 (s, 1H), 9.40 (d, *J* = 16.9 Hz, 1H), 8.67 (s, 1H), 8.25 (d, *J* = 23.5 Hz, 1H), 7.88 (d, *J* = 11.3 Hz, 1H), 7.65 (d, *J* = 21.8 Hz, 1H), 7.44 (s, 1H), 7.29 (d, *J* = 11.9 Hz, 1H), 6.99 (s, 1H), 6.84 (s, 1H), 6.46–6.33 (m, 1H), 5.33 (s, 1H). <sup>13</sup>C NMR (101 MHz, DMSO-*d*<sub>6</sub>)  $\delta$  169.34, 160.28, 151.89, 145.03, 139.34, 139.21, 129.18, 129.10 (2C), 126.71, 126.53 (2C), 125.16, 124.55, 121.11, 120.88, 120.24, 116.79, 115.78, 115.19, 110.04, 108.65. IR (KBr)  $\text{cm}^{-1}$ : 3445, 3100, 1685, 1606, 1560, 1485, 1321, 1200. TOF MS ES+ ( $m/z$ ): [M + H]<sup>+</sup>, calcd for C<sub>22</sub>H<sub>12</sub>BrF<sub>2</sub>N<sub>7</sub>O<sub>3</sub>: 540.0231, found, 540.0232. HPLC purity: 97.06% (Column: Dikma Luna C18; Mobile phase: H<sub>2</sub>O:MeCN = 60:40; Column temperature: 26 °C; Wavelength: 280 nm; Flow rate: 1.0 mL/min).

***N*-(4-([1,2,4]triazolo[4,3-*a*]pyrazin-8-yl)oxy)-3-fluorophenyl)-1-(4-methoxyphenyl)-4-oxo-1,4-dihydropyridazine-3-carboxamide (21k).**

Brown solid in 31.2% yield. m.p: 295.6–298.3 °C. <sup>1</sup>H NMR (400 MHz, DMSO-*d*<sub>6</sub>)  $\delta$  12.09 (s, 1H), 9.41 (d, *J* = 12.1 Hz, 1H), 8.86 (s, 1H), 8.28 (s, 1H), 7.88 (s, 1H), 7.65 (s, 2H), 7.45 (s, 1H), 7.31 (s, 1H), 7.08 (s, 2H), 6.86 (s, 1H), 6.57 (s, 1H), 3.77 (s, 3H). <sup>13</sup>C NMR (101 MHz, DMSO-*d*<sub>6</sub>)  $\delta$  169.66, 160.45, 152.31, 147.36, 142.52, 142.43, 139.33, 136.93, 128.45, 126.58 (2C), 126.55, 125.16, 123.54 (2C), 121.23, 118.83, 115.78, 115.22 (2C), 110.71, 108.863, 56.16. IR (KBr)  $\text{cm}^{-1}$ : 3441, 3029, 1693, 1594, 1569, 14511, 1325, 1203. TOF MS ES+ ( $m/z$ ): [M + H]<sup>+</sup>, calcd for C<sub>23</sub>H<sub>16</sub>FN<sub>7</sub>O<sub>4</sub>: 474.1326, found, 474.1326. HPLC purity: 98.26% (Column: Dikma Luna C18; Mobile phase:

H<sub>2</sub>O:MeCN = 70:30; Column temperature: 26 °C; Wavelength: 280 nm; Flow rate: 1.0 mL/min).

***N-(4-([1,2,4]triazolo[4,3-*a*]pyrazin-8-yl)oxy)-3-fluorophenyl)-1-(4-fluorophenyl)-4-oxo-1,4-dihydropyridazine-3-carboxamide (21l).***

White solid in 42.1% yield. m.p: 300.5–302.4 °C. <sup>1</sup>H NMR (400 MHz, DMSO-*d*<sub>6</sub>) δ 11.96 (s, 1H), 9.42 (s, 1H), 8.90 (d, *J* = 8.0 Hz, 1H), 8.29 (s, 1H), 7.88 (d, *J* = 12.5 Hz, 1H), 7.79 (s, 2H), 7.47–7.37 (m, 4H), 7.31 (d, *J* = 4.7 Hz, 1H), 6.86 (d, *J* = 8.0 Hz, 1H). <sup>13</sup>C NMR (101 MHz, DMSO-*d*<sub>6</sub>) δ 169.19, 162.84, 159.89, 151.41, 147.32, 142.07, 139.47, 138.84, 137.17, 126.04 (2C), 124.67, 123.96 (2C), 123.87, 120.52, 116.62 (2C), 116.39, 116.27, 115.29, 108.39. IR (KBr) cm<sup>-1</sup>: 3441, 3108, 1699, 1595, 1565, 1509, 1328, 1203. TOF MS ES+ (*m/z*): [M + H]<sup>+</sup>, calcd for C<sub>22</sub>H<sub>13</sub>F<sub>2</sub>N<sub>7</sub>O<sub>3</sub>: 462.1126, found, 462.1125. HPLC purity: 99.99% (Column: Dikma Luna C18; Mobile phase: H<sub>2</sub>O:MeCN = 70:30; Column temperature: 26 °C; Wavelength: 280 nm; Flow rate: 1.0 mL/min).

***N-(4-((3-methyl-[1,2,4]triazolo[4,3-*a*]pyrazin-8-yl)oxy)phenyl)-4-oxo-1-phenyl-1,4-dihydropyridazine-3-carboxamide (22a).***

Grayish white solid in 49.2% yield. m.p: 289.4–293.9 °C. <sup>1</sup>H NMR (400 MHz, DMSO-*d*<sub>6</sub>) δ 11.85 (s, 1H), 8.93 (d, *J* = 8.0 Hz, 1H), 8.10 (s, 1H), 7.77–7.64 (m, 4H), 7.60–7.40 (m, 4H), 7.28 (d, *J* = 7.0 Hz, 2H), 6.85 (d, *J* = 8.2 Hz, 1H), 2.66 (s, 3H). <sup>13</sup>C NMR (101 MHz, DMSO-*d*<sub>6</sub>) δ 169.66, 159.41, 146.05, 142.59, 141.51, 129.49 (2C), 128.57 (2C), 128.37, 125.54, 122.24, 121.34 (2C), 121.18, 120.76, 120.23 (2C), 119.42, 115.19, 113.21, 108.53, 9.61. IR (KBr) cm<sup>-1</sup>: 3441, 3089, 1688, 1592, 1563, 1488, 1329, 1216. TOF MS ES+ (*m/z*): [M + H]<sup>+</sup>, calcd for C<sub>23</sub>H<sub>17</sub>N<sub>7</sub>O<sub>3</sub>: 440.1471, found, 440.1472. HPLC purity: 99.42% (Column: Dikma Luna C18; Mobile phase: H<sub>2</sub>O:MeCN = 70:30; Column temperature: 26 °C; Wavelength: 280 nm; Flow rate: 1.0 mL/min).

***1-(3-chloro-4-fluorophenyl)-N-(4-((3-methyl-[1,2,4]triazolo[4,3-*a*]pyrazin-8-yl)oxy)phenyl)-4-oxo-1,4-dihydropyridazine-3-carboxamide (22b).***

Brown solid in 51.2% yield. m.p: 248.0–251.3 °C. <sup>1</sup>H NMR (400 MHz, DMSO-*d*<sub>6</sub>) δ 11.76 (s, 1H), 8.95 (m, 1H), 8.16 (s, 1H), 8.09 (s, 1H), 7.72 (d, *J* = 8.8 Hz, 3H), 7.57 (s, 1H), 7.29 (d, *J* = 9.0 Hz, 3H), 6.83 (s, 1H), 2.66 (s, 3H). <sup>13</sup>C NMR (101 MHz, DMSO-*d*<sub>6</sub>) δ 169.93, 159.61, 149.59, 143.18, 140.20, 137.24, 135.24 (2C), 126.80, 125.90, 124.48 (2C), 123.04, 122.97, 120.80, 119.71 (2C), 118.41 (2C), 118.19, 116.07, 108.21, 12.66. IR (KBr) cm<sup>-1</sup>: 3441, 3043, 1687, 1601, 1560, 1490, 1329, 1201. TOF MS ES+ (*m/z*): [M + H]<sup>+</sup>, calcd for C<sub>23</sub>H<sub>15</sub>ClFN<sub>7</sub>O<sub>3</sub>: 492.0987, found, 492.0989. HPLC purity: 98.54% (Column: Dikma Luna C18; Mobile phase: H<sub>2</sub>O:MeCN = 50:50; Column temperature: 26 °C; Wavelength: 280 nm; Flow rate: 1.0 mL/min).

***1-(4-chloro-3-(trifluoromethyl)phenyl)-N-(4-((3-methyl-[1,2,4]triazolo[4,3-*a*]pyrazin-8-yl)oxy)phenyl)-4-oxo-1,4-dihydropyridazine-3-carboxamide (22c).***

Brown solid in 33.2% yield. m.p: 257.6–259.8 °C. <sup>1</sup>H NMR (400 MHz, DMSO-*d*<sub>6</sub>) δ 11.72 (s, 1H), 8.70 (d, *J* = 8.1

Hz, 1H), 8.22 (s, 1H), 8.11 (s, 1H), 8.03 (s, 1H), 7.93 (d,  $J = 8.4$  Hz, 2H), 7.80 (d,  $J = 8.7$  Hz, 1H), 7.74 (d,  $J = 8.1$  Hz, 1H), 7.28 (d,  $J = 7.2$  Hz, 2H), 6.29 (d,  $J = 8.1$  Hz, 1H), 2.66 (s, 3H).  $^{13}\text{C}$  NMR (101 MHz, DMSO- $d_6$ )  $\delta$  169.85, 159.87, 153.04, 148.36, 142.17, 142.13, 139.08 (2C), 136.24, 133.49 (2C), 130.76, 128.22, 127.86, 127.17, 126.69, 124.11, 122.94 (2C), 121.44 (2C), 120.59, 115.04, 10.35. IR (KBr)  $\text{cm}^{-1}$ : 3444, 3088, 1692, 1600, 1561, 1490, 132, 1191. TOF MS ES+ ( $m/z$ ):  $[\text{M} + \text{H}]^+$ , calcd for  $\text{C}_{24}\text{H}_{15}\text{ClF}_3\text{N}_7\text{O}_3$ : 542.0955, found, 542.0953. HPLC purity: 97.49% (Column: Dikma Luna C18; Mobile phase:  $\text{H}_2\text{O}:\text{MeCN} = 50:50$ ; Column temperature: 26 °C; Wavelength: 280 nm; Flow rate: 1.0 mL/min).

***1-(4-bromo-2-fluorophenyl)-N-(4-((3-methyl-[1,2,4]triazolo[4,3-a]pyrazin-8-yl)oxy)phenyl)-4-oxo-1,4-dihydropyridazine-3-carboxamide (22d).***

Light yellow solid in 31.2% yield. m.p: 286.3–298.5 °C.  $^1\text{H}$  NMR (400 MHz, DMSO- $d_6$ )  $\delta$  11.71 (s, 1H), 8.78 (s, 1H), 7.93 (s, 1H), 7.75 (s, 1H), 7.61 (d,  $J = 8.6$  Hz, 3H), 7.52 (s, 1H), 7.30 (s, 3H), 6.79 (s, 1H), 2.65 (s, 3H).  $^{13}\text{C}$  NMR (101 MHz, DMSO- $d_6$ )  $\delta$  170.11, 160.67, 154.53, 149.11, 145.65, 143.91, 140.15 (2C), 136.98, 129.87 (2C), 129.63, 129.52, 126.95, 123.65 (2C), 122.17 (2C), 121.58, 120.79, 116.71, 114.65, 11.04. IR (KBr)  $\text{cm}^{-1}$ : 3439, 3032, 1693, 1605, 1563, 1502, 1329, 1215. TOF MS ES+ ( $m/z$ ):  $[\text{M} + \text{H}]^+$ , calcd for  $\text{C}_{23}\text{H}_{15}\text{BrFN}_7\text{O}_3$ : 536.0482, found, 536.0482. HPLC purity: 98.60% (Column: Dikma Luna C18; Mobile phase:  $\text{H}_2\text{O}:\text{MeCN} = 60:40$ ; Column temperature: 26 °C; Wavelength: 280 nm; Flow rate: 1.0 mL/min).

***1-(4-methoxyphenyl)-N-(4-((3-methyl-[1,2,4]triazolo[4,3-a]pyrazin-8-yl)oxy)phenyl)-4-oxo-1,4-dihydropyridazine-3-carboxamide (22e).***

Light yellow solid in 52.7% yield. m.p: 298.8–301.2 °C.  $^1\text{H}$  NMR (400 MHz, DMSO- $d_6$ )  $\delta$  11.93 (s, 1H), 9.03 (s, 2H), 8.20 (s, 1H), 7.79 (d,  $J = 27.6$  Hz, 4H), 7.56 (d,  $J = 37.1$  Hz, 4H), 7.36 (s, 2H), 6.90 (s, 2H), 2.74 (s, 3H).  $^{13}\text{C}$  NMR (101 MHz, DMSO- $d_6$ )  $\delta$  169.84, 160.15, 153.18, 148.19, 146.78, 143.42, 142.24 (2C), 136.35, 130.21 (2C), 130.17, 129.10, 129.00, 126.26, 122.98, 121.90 (2C), 121.46 (2C), 120.95, 113.93, 55.61, 10.33. IR (KBr)  $\text{cm}^{-1}$ : 3441, 3041, 1688, 1592, 1562, 1502, 1329, 1216. TOF MS ES+ ( $m/z$ ):  $[\text{M} + \text{H}]^+$ , calcd for  $\text{C}_{24}\text{H}_{19}\text{N}_7\text{O}_4$ : 470.1577, found, 470.1572. HPLC purity: 99.11% (Column: Dikma Luna C18; Mobile phase:  $\text{H}_2\text{O}:\text{MeCN} = 70:30$ ; Column temperature: 26 °C; Wavelength: 280 nm; Flow rate: 1.0 mL/min).

***1-(4-fluorophenyl)-N-(4-((3-methyl-[1,2,4]triazolo[4,3-a]pyrazin-8-yl)oxy)phenyl)-4-oxo-1,4-dihydropyridazine-3-carboxamide (22f).***

Yellow solid in 53.5% yield. m.p: 280.1–283.4 °C.  $^1\text{H}$  NMR (400 MHz, DMSO- $d_6$ )  $\delta$  11.85 (s, 1H), 8.90 (s, 1H), 8.52 (s, 1H), 8.10 (s, 1H), 7.80–7.72 (m, 3H), 7.61 (s, 1H), 7.40 (s, 1H), 7.29 (s, 2H), 6.85 (d,  $J = 8.3$  Hz, 1H), 6.27 (s, 1H), 2.66 (s, 3H).  $^{13}\text{C}$  NMR (101 MHz, DMSO- $d_6$ )  $\delta$  169.80, 160.05, 153.19, 148.03, 146.77, 142.49, 140.02 (2C),

139.46, 136.32, 126.26, 124.46 (2C), 124.37, 122.99 (2C), 121.47 (2C), 120.90, 117.10, 116.87, 113.92, 110.32. IR (KBr)  $\text{cm}^{-1}$ : 3440, 3082, 1688, 1602, 1563, 1487, 1330, 1216. TOF MS ES+ ( $m/z$ ):  $[\text{M} + \text{H}]^+$ , calcd for  $\text{C}_{23}\text{H}_{16}\text{FN}_7\text{O}_3$ : 458.1377, found, 458.1374. HPLC purity: 97.41% (Column: Dikma Luna C18; Mobile phase:  $\text{H}_2\text{O}:\text{MeCN} = 70:30$ ; Column temperature: 26 °C; Wavelength: 280 nm; Flow rate: 1.0 mL/min).

***N-(3-fluoro-4-((3-methyl-[1,2,4]triazolo[4,3-a]pyrazin-8-yl)oxy)phenyl)-4-oxo-1-phenyl-1,4-dihydropyridazine-3-carboxamide (22g).***

Brown solid in 37.2% yield. m.p: 261.9–262.1 °C.  $^1\text{H}$  NMR (400 MHz,  $\text{DMSO}-d_6$ )  $\delta$  12.01 (s, 1H), 8.95 (d,  $J = 7.7$  Hz, 1H), 8.16 (s, 1H), 7.88 (d,  $J = 12.6$  Hz, 1H), 7.74 (d,  $J = 7.9$  Hz, 2H), 7.54 (d,  $J = 8.1$  Hz, 2H), 7.44 (s, 3H), 7.31 (s, 1H), 6.86 (d,  $J = 7.7$  Hz, 1H), 2.67 (s, 3H).  $^{13}\text{C}$  NMR (101 MHz,  $\text{DMSO}-d_6$ )  $\delta$  169.73, 160.46, 151.99, 147.01, 143.38, 142.30, 130.21 (2C), 129.94, 129.12 (2C), 125.99, 125.12 (2C), 121.87 (2C), 121.06, 120.74, 116.76, 114.61, 108.86, 108.63, 10.35. IR (KBr)  $\text{cm}^{-1}$ : 3444, 3048, 1689, 1604, 1567, 1489, 1331, 1214. TOF MS ES+ ( $m/z$ ):  $[\text{M} + \text{H}]^+$ , calcd for  $\text{C}_{23}\text{H}_{16}\text{FN}_7\text{O}_3$ : 458.1377, found, 458.1371. HPLC purity: 96.30% (Column: Dikma Luna C18; Mobile phase:  $\text{H}_2\text{O}:\text{MeCN} = 70:30$ ; Column temperature: 26 °C; Wavelength: 280 nm; Flow rate: 1.0 mL/min).

***1-(3-chloro-4-fluorophenyl)-N-(3-fluoro-4-((3-methyl-[1,2,4]triazolo[4,3-a]pyrazin-8-yl)oxy)phenyl)-4-oxo-1,4-dihydropyridazine-3-carboxamide (22h).***

Brown solid in 47.2% yield. m.p: 298.7–301.4 °C.  $^1\text{H}$  NMR (400 MHz,  $\text{DMSO}-d_6$ )  $\delta$  11.88 (s, 1H), 8.13 (s, 1H), 8.05 (s, 1H), 7.87 (d,  $J = 12.1$  Hz, 1H), 7.78 (s, 1H), 7.60 (s, 2H), 7.45 (s, 2H), 7.30 (s, 1H), 6.85 (s, 1H), 2.67 (s, 3H).  $^{13}\text{C}$  NMR (101 MHz,  $\text{DMSO}-d_6$ )  $\delta$  169.65, 160.33, 151.99, 147.07, 142.46, 140.25, 138.91 (2C), 126.01, 125.13, 124.40 (2C), 122.94, 122.86 (2C), 120.81 (2C), 118.44, 118.22, 116.82, 114.63, 108.90, 10.36. IR (KBr)  $\text{cm}^{-1}$ : 3439, 3039, 1690, 1604, 1565, 1498, 1333, 1219. TOF MS ES+ ( $m/z$ ):  $[\text{M} + \text{H}]^+$ , calcd for  $\text{C}_{23}\text{H}_{14}\text{ClF}_2\text{N}_7\text{O}_3$ : 510.0893, found, 510.0893. HPLC purity: 96.61% (Column: Dikma Luna C18; Mobile phase:  $\text{H}_2\text{O}:\text{MeCN} = 50:50$ ; Column temperature: 26 °C; Wavelength: 280 nm; Flow rate: 1.0 mL/min).

***1-(4-chloro-3-(trifluoromethyl)phenyl)-N-(3-fluoro-4-((3-methyl-[1,2,4]triazolo[4,3-a]pyrazin-8-yl)oxy)phenyl)-4-oxo-1,4-dihydropyridazine-3-carboxamide (22i).***

Light yellow solid in 45.2% yield. m.p: 311.2–313.0 °C.  $^1\text{H}$  NMR (400 MHz,  $\text{DMSO}-d_6$ )  $\delta$  11.84 (s, 1H), 9.02 (s, 1H), 8.21 (s, 1H), 8.10 (d,  $J = 22.5$  Hz, 2H), 7.88 (d,  $J = 19.2$  Hz, 2H), 7.44 (s, 2H), 7.30 (s, 1H), 6.88 (s, 1H), 2.67 (s, 3H).  $^{13}\text{C}$  NMR (101 MHz,  $\text{DMSO}-d_6$ )  $\delta$  169.79, 160.22, 151.99, 148.26, 142.36, 142.16, 138.91, 137.57, 135.20, 133.57 (2C), 131.08, 127.27, 126.00 (2C), 125.16, 121.41, 120.77 (2C), 116.82, 114.65 (2C), 108.91, 10.37. IR (KBr)  $\text{cm}^{-1}$ : 3443, 3086, 1707, 1598, 1564, 1489, 1326, 1219. TOF MS ES+ ( $m/z$ ):  $[\text{M} + \text{H}]^+$ , calcd for  $\text{C}_{24}\text{H}_{14}\text{ClF}_4\text{N}_7\text{O}_3$ : 560.0861, found, 560.0865. HPLC purity: 97.38% (Column: Dikma Luna C18; Mobile phase:  $\text{H}_2\text{O}:\text{MeCN} = 50:50$ ; Column

temperature: 26 °C; Wavelength: 280 nm; Flow rate: 1.0 mL/min).

View Article Online  
DOI: 10.1039/D0NJ00575D

***1-(4-bromo-2-fluorophenyl)-N-(3-fluoro-4-((3-methyl-[1,2,4]triazolo[4,3-a]pyrazin-8-yl)oxy)phenyl)-4-oxo-1,4-dihydropyridazine-3-carboxamide (22j).***

Grayish white solid in 33.2% yield. m.p: 290.7–292.5 °C. <sup>1</sup>H NMR (400 MHz, DMSO-*d*<sub>6</sub>) δ 11.77 (s, 1H), 8.34 (d, *J* = 7.8 Hz, 1H), 7.79 (d, *J* = 10.5 Hz, 1H), 7.63 (s, 1H), 7.53 (s, 3H), 7.43 (s, 1H), 7.31 (s, 1H), 6.35 (d, *J* = 7.8 Hz, 1H), 5.67 (s, 1H), 2.67 (s, 3H). <sup>13</sup>C NMR (101 MHz, DMSO-*d*<sub>6</sub>) δ 170.08, 160.76, 147.36, 142.63, 139.24, 138.07 (2C), 137.16, 130.54 (2C), 129.46, 128.77, 126.33, 125.45, 122.21 (2C), 121.41 (2C), 117.09, 114.93, 109.21, 108.97, 10.68. IR (KBr) cm<sup>-1</sup>: 3442, 3053, 1686, 1610, 1565, 1486, 1327, 1210. TOF MS ES+ (*m/z*): [M + H]<sup>+</sup>, calcd for C<sub>23</sub>H<sub>14</sub>BrF<sub>2</sub>N<sub>7</sub>O<sub>3</sub>: 554.0388, found, 554.0388. HPLC purity: 98.65% (Column: Dikma Luna C18; Mobile phase: H<sub>2</sub>O:MeCN = 60:40; Column temperature: 26 °C; Wavelength: 280 nm; Flow rate: 1.0 mL/min).

***N-(3-fluoro-4-((3-methyl-[1,2,4]triazolo[4,3-a]pyrazin-8-yl)oxy)phenyl)-1-(4-methoxyphenyl)-4-oxo-1,4-dihydropyridazine-3-carboxamide (22k).***

White solid in 41.8% yield. m.p: 301.7–307.5 °C. <sup>1</sup>H NMR (400 MHz, DMSO-*d*<sub>6</sub>) δ 12.16 (s, 1H), 9.14 (s, 1H), 8.35 (s, 1H), 8.07 (d, *J* = 11.9 Hz, 1H), 7.92 (s, 3H), 7.69 (d, *J* = 43.0 Hz, 5H), 7.50 (s, 1H), 7.05 (s, 1H), 2.86 (s, 3H). <sup>13</sup>C NMR (101 MHz, DMSO-*d*<sub>6</sub>) δ 168.50, 160.25, 151.99, 147.06, 143.31, 138.91 (2C), 129.11, 128.96, 128.83 (2C), 126.00 (2C), 125.12, 120.89 (2C), 120.66, 120.23, 116.77, 116.20, 114.63, 108.65, 55.36, 10.36. IR (KBr) cm<sup>-1</sup>: 3442, 3051, 1689, 1604, 1567, 1489, 1331, 1214. TOF MS ES+ (*m/z*): [M + H]<sup>+</sup>, calcd for C<sub>24</sub>H<sub>18</sub>FN<sub>7</sub>O<sub>4</sub>: 488.1483, found, 488.1480. HPLC purity: 99.71% (Column: Dikma Luna C18; Mobile phase: H<sub>2</sub>O:MeCN = 70:30; Column temperature: 26 °C; Wavelength: 280 nm; Flow rate: 1.0 mL/min).

***N-(3-fluoro-4-((3-methyl-[1,2,4]triazolo[4,3-a]pyrazin-8-yl)oxy)phenyl)-1-(4-fluorophenyl)-4-oxo-1,4-dihydropyridazine-3-carboxamide (22l).***

Brown solid in 36.2% yield. m.p: 289.5–295.1 °C. <sup>1</sup>H NMR (400 MHz, DMSO-*d*<sub>6</sub>) δ 11.72 (s, 1H), 8.99 (s, 1H), 8.64 (s, 1H), 8.24 (s, 1H), 7.96 (s, 1H), 7.87 (s, 1H), 7.71 (s, 2H), 7.47 (s, 2H), 7.38 (s, 1H), 6.94 (s, 1H), 2.76 (s, 3H). <sup>13</sup>C NMR (101 MHz, DMSO-*d*<sub>6</sub>) δ 170.37, 161.11, 152.70, 148.58, 147.76, 143.24, 140.67 (2C), 139.61, 126.71, 125.81, 125.14, 125.05 (2C), 121.69, 117.81 (2C), 117.57 (2C), 117.47, 115.31, 109.60, 11.06. IR (KBr) cm<sup>-1</sup>: 3443, 3089, 1692, 1604, 1569, 1487, 1331, 1214. TOF MS ES+ (*m/z*): [M + H]<sup>+</sup>, calcd for C<sub>23</sub>H<sub>15</sub>F<sub>2</sub>N<sub>7</sub>O<sub>3</sub>: 476.1283, found, 476.1282. HPLC purity: 98.49% (Column: Dikma Luna C18; Mobile phase: H<sub>2</sub>O:MeCN = 70:30; Column temperature: 26 °C; Wavelength: 280 nm; Flow rate: 1.0 mL/min).

### 3.3 Anti-tumor assay

The anti-tumor activities of target compounds (**21a-l** and **22a-l**) were evaluated with A549, MCF-7 and Hela cell

lines by the standard MTT assay *in vitro*, with Foretinib as positive control. Specific operations were based on our previous research <sup>11</sup>.

### 3.4 Cell apoptosis assay by flow cytometry

A549 cells were seeded in a 6-well plate at  $1 \times 10^5$  cells per well and incubated for 24 h, and then treated with compound **22i** for 72 h. Cells were harvested and fixed with ice-cold 70% ethanol at 4 °C for 12 h, and then ethanol was removed and the cells were washed with cold PBS. Cells were then incubated in 0.5 mL of PBS containing 1 mg/mL Rnase for 30 min at 37 °C. After which, the cells were stained with propidium iodide (PI) in the dark for 30 min. Finally, the DNA contents were measured by flow cytometer.

### 3.5 Kinase selectivity assay

The most compounds were tested for their activity against c-Met through the mobility shift assay, with Foretinib being positive controls. Specific operations were based on according to our previous research <sup>16</sup>.

### 3.6 Acridine orange single staining

The cancer cell apoptotic of target compound **22i** were evaluated with A549 cancer cell line by acridine orange single staining. Specific operations were based on according to our previous research <sup>18</sup>.

### 3.7 Molecular docking study

The co-crystal structure of c-Met (PDB code 3LQ8) was chosen as the template to generate the docking modes. For the preparation of ligands, the 3D structures were generated and their energy minimizations were performed by AutoDock 4.2 software (The Scripps Research Institute, USA). After the protein preparation process of flexible docking, the whole c-Met was defined as a receptor and compound **22i** was placed during the molecular docking procedure. Types of interactions of the docked c-Met with ligand was analyzed and then the docking conformations was selected and saved based on calculated energy. All the docking results were processed and modified in PyMOL 1.8.x software (<https://pymol.org>).

## 4 Conclusions

In summary, based on the structure based drug design (SBDD) strategy and bioisosterism principles, a series of [1,2,4]triazolo[4,3-*a*]pyrazine derivatives bearing 4-oxo-pyridazinone moiety as potential c-Met kinase inhibitors were designed and evaluated for the IC<sub>50</sub> values against three cancer cell lines (A549, MCF-7 and Hela). Most compounds were selected to evaluate for the activity against c-Met kinase. Among them, the most promising compound **22i** showed superior anti-tumor activity for A549, MCF-7 and Hela cell lines with IC<sub>50</sub> values of  $0.83 \pm 0.07 \mu\text{M}$ ,  $0.15 \pm 0.08 \mu\text{M}$  and  $2.85 \pm 0.74 \mu\text{M}$ , respectively, which also possessed excellent c-Met kinase inhibition on nanomolar level (IC<sub>50</sub> = 48

nM). According to the result of AO single staining and cell apoptosis assay, it claimed that compound **22i** could induce remarkable apoptosis of A549 cells in a dose-dependent manner. Furthermore, compound **22i** could stimulate A549 cells arrest at G0/G1 phase. By far, the data indicated that compound **22i** may be a potential c-Met kinase inhibitor and further research will be carried out to identify more anti-tumor mechanisms.

## 5 Conflicts of interest

There are no conflicts to declare.

## 6 Acknowledgments

We gratefully acknowledge the generous support provided by The National Natural Science Funds of China (No. 21662014, No. 21967009), Natural Science Foundation of Jiangxi, China (20181BBG70003, 20181ACB20025, 20192BAB215061), Science and Technology Project Founded by the Education Department of Jiangxi Province, China (GJJ190583).

## 7 References

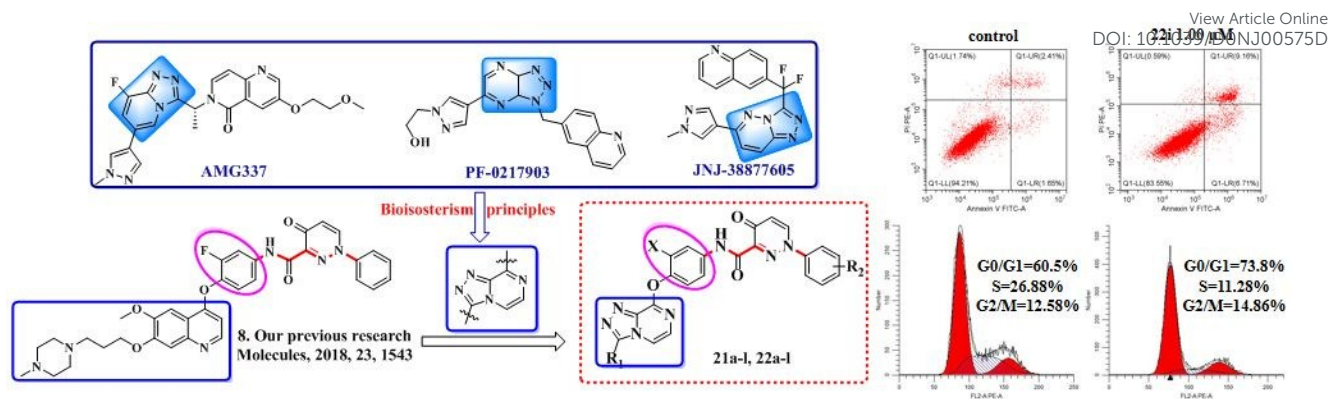
1. W. Zhu, W. Wang, S. Xu, J. Wang, Q. Tang, C. Wu, Y. Zhao and P. Zheng, *Bioorg. Med. Chem.*, 2016, **24**, 1749-1756.
2. C. Li, J. Wu, M. Hynes, J. Dosch, B. Sarkar, T.H. Welling, M. Magliano and D.M. Simeone, *Gastroenterology*, 2011, **141**, 2218-2227.
3. W.K. You, B. Sennino, C.W. Williamson, B. Falcón, H. Hashizume, L.C Yao, D.T. Aftab and D.M. McDonald, *Cancer Res.*, 2011, **71**, 4758-4768.
4. T.K. Choueiri, S.K. Pal, D.F. McDermott, S. Morrissey, K.C. Ferguson, J. Holland, W. G. Kaelin and J. P. Dutcher, *Ann. Oncol.*, 2014, **25**, 1603-1608.
5. M. Zillhardt, S. Park, I. Romero, K. Sawada, A. Montag, T. Krausz, S. Yamada, M. Peter and E. Clin, *Cancer Res.*, 2011, **17**, 4042-4051.
6. P.E. Hughes, K. Rex, S. Caenepeel, Y. Yang, Y. Zhang, M.A. Broome, H.T. Kha, T.L Burgess, B. Amore, P.J. Kaplan-Lefko, J. Moriguchi, J. Werner, M.A. Damore, D. Baker, D.M. Choquette, J. Harmange, R. Radinsky, R. Kendall, I. Dussault and A. Coxon, *Molecular Cancer Therapeutics*, 2016, **15**, 1568-1579.
7. L. Liu, M.H. Norman, M. Lee, N. Xi, A. Siegmund, A.A. Boezio, S. Booker, D. Choquette, N.D. D'Angelo, J. Germain, K. Yang, Y. Yang, Y. Zhang, S.F. Bellon, D.A. Whittington, J. Harmange, C. Dominguez, T. Kim and I. Dussault, *J. Med. Chem.*, **55**, 1868-1897.
8. W. Wang, S. Xu, Y. Duan, X. Liu, X. Li, C. Wang, B. Zhao, P. Zheng and W. Zhu, *Eur. J. Med. Chem.*, 2018,

1  
2  
3  
4  
5  
6  
7  
8  
9  
10  
11  
12  
13  
14  
15  
16  
17  
18  
19  
20  
21  
22  
23  
24  
25  
26  
27  
28  
29  
30  
31  
32  
33  
34  
35  
36  
37  
38  
39  
40  
41  
42  
43  
44  
45  
46  
47  
48  
49  
50  
51  
52  
53  
54  
55  
56  
57  
58  
59  
60

145, 315-327.

View Article Online  
DOI: 10.1039/D0NJ00575D

9. Q. Tang, L. Wang, Y. Tu, W. Zhu, R. Luo, Q. Tu, P. Wang, C. Wu, P. Gong and P. Zheng, *Bioorg. Med. Chem. Lett.*, 2016, **26**, 1680-1684.
10. L. Wang, X. Liu, Y. Duan, X. Li, B. Zhao, C. Wang, Z. Xiao, P. Zheng, Q. Tang, W. Zhu, *Chem. Bio. Drug Des.*, 2018, **92**, 1301-1314.
11. L. Wang, X. Liu, S. Xu, Q. Tang, Y. Duan, Z. Xiao, J. Zhi, L. Jiang, P. Zheng and W. Zhu, *Eur. J. Med. Chem.*, 2017, **141**, 538-551.
12. H. Robert L. and Z. Allison L. WO Pat., 2015100117A1, 2015.
13. M. Naoki, M. Shigemitsu, and I. Shinichi, WO Pat., 2009136663, 2009.
14. W. Vaccaro, Z. Chen, D. Dodd, T. Huynh, J. Lin, C. Liu, C. Mussari, J. Tokarski, D. Tortolani, S. Wroblewski and S. Lin, US Pat., 20080045536A1, 2008.
15. M. Naoki, M. Shigemitsu, and I. Shinichi, WO Pat., 2009096435A1, 2009.
16. X. Liu, J. Kou, Z. Xiao, F. Tian, J. Hu, P. Zheng and W. Zhu, *Molecules*, 2018, **23**, 1543.
17. L. Wang, S. Xu, X. Chen, X. Liu, Y. Duan, D. Kong, D. Zhao, P. Zheng, Q. Tang and W. Zhu, *Bioorg Med Chem*, 2018, **26**, 245-256.
18. L. Wang, S. Xu, X. Liu, X. Chen, H. Xiong, S. Hou, W. Zou, Q. Tang, P. Zheng and W. Zhu, *Bioorg. Chem.*, 2018, **77**, 370-380.



we disclosed the preparation and biological evaluation of a series of [1,2,4]triazolo[4,3-*a*]pyrazine derivatives bearing 4-oxo-pyridazinone moiety, which demonstrated potent inhibition of c-Met kinase, culminating in the discovery of **22i**.